ARTICLE

Phase Transition of Poly(acrylic acid-co-N-isopropylacrylamide) Core-shell Nanogels

Xiao-bing Liu, Jian-feng Zhou, Xiao-dong Ye*

Hefei National Laboratory for Physical Sciences at the Microscale, Department of Chemical Physics, University of Science and Technology of China, Hefei 230026, China

(Dated: Received on April 28, 2012; Accepted on May 9, 2012)

A series of poly(acrylic acid) macromolecular chain transfer agents with different molecular weights were synthesized by reversible addition-fragmentation chain transfer (RAFT) polymerization and characterized by ^{1}H NMR and gel permeation chromatography. Multiresponsive core-shell nanogels were prepared by dispersion polymerization of N-isopropylacrylamide in water using these poly(potassium acrylate) macro-RAFT agents as the electrosteric stabilizer. The size of the nanogels decreases with the amount of the macro-RAFT agent, indicating that the surface area occupied by per polyelectrolyte group is a critical parameter for stabilizing the nanogels. The volume phase transition and the zeta potentials of the nanogels in aqueous solutions were studied by dynamic light scattering and zetasizer analyzer, respectively.

Key words: Core-shell nanogel, Dispersion polymerization, Multiresponsive, Phase transition

I. INTRODUCTION

Recently polymeric nanogels have received much more attention because of the numerous useful applications, including in the health care, coating, or the pharmaceutical industry [1]. Particularly, thermally responsive nano/micro-sized gels based on N-isopropylacrylamide monomer have potential use in optical/electronic devices, biomedical applications, and responsive surfaces [2−7]. Poly(N-isopropylacrylamide) (PNIPAM) nano/microgels exhibit a remarkable phase transition at the lower critical solution temperature (LCST≈32 °C) in aqueous solution [8−11]. The nano/microgels swell and shrink below and above the LCST, respectively.

The synthesis of thermally responsive colloidal microgels in water can provide both industrial and environmental benefits. It relies on a free-radical dispersion polymerization process in aqueous solution [12]. Above the LCST of the thermally sensitive polymers in water, nanoparticles form in the solution, the stability of which is ensured by either an added surfactant, ionic groups or neutral water-soluble polymers incorporated into the polymer chains during the polymerization. Recently, radical copolymerization of a vinylic monomer and a bifunctional comonomer in surfactant-free aqueous dispersion in the presence of a macroinitiator or a macromolecular chain transfer agent has received great interest [13−18]. For example, Armes *et al.* have prepared nanoparticles with poly(potassium 3-sulfopropyl methacrylate) in the shell using a reversible addition-fragmentation chain transfer (RAFT) aqueous dispersion polymerization [16]. Throughout RAFT dispersion polymerization of styrene in methanol, He *et al.* have synthesized poly(acrylic acid)-*b*-polystyrene diblock copolymers (PAA-*b*-PS) and investigated the assembly behavior [17]. However, to our best knowledge, through this method core-shell nanogels with both pH sensitivity and thermosensitivity have not been reported before. In the present work, we report a facile procedure to prepare pH and temperature sensitive PNIPAM nanogels with poly(potassium acrylate)(PAA-K) in the shell through a free-radical aqueous dispersion polymerization using trithiocarbonated PAA-K as the reactive stabilizer. Poly(acrylic acid) (PAA) precursor chains were obtained by RAFT polymerization and readily converted into PAA-K via adding K_2CO_3. By using dynamic laser light scattering and zetasizer analyzer, we have investigated the phase transition and zeta potentials of the nanogels in aqueous solutions.

II. EXPERIMENTS

A. Materials

Acrylic acid (AA, Shanghai Chem., 96%) was dried over anhydrous magnesium sulfate and then distilled under reduced pressure prior to use. Azobis(isobutyronitrile) (AIBN, Aldrich, 99%) was recrystallized from ethanol and dried. 1,4-dioxane (99%) was

*Author to whom correspondence should be addressed. E-mail: xdye@ustc.edu.cn

TABLE I Recipes and results for the synthesis of PAA macro-CTA via RAFT polymerization in dioxane at 80 °C with 10.00 g of AA, 20.0 mL of 1,4-dioxane, different amounts of AIBN and DMP as the initiator and the chain transfer agent, respectively.

Entry No.	AIBN/mg	DMP/g	T/°C	M_n[a]/(g/mol)	M_w/M_n[a]	M_n[b]/(g/mol)
1	16	3.64	80	5000	1.10	2000
2	13	2.46	80	8200	1.09	3800
3	7	1.23	80	9400	1.08	4500

[a] Measured by GPC in water with PEO calibration.
[b] Measured by NMR.

refluxed several hours and freshly distilled from sodium benzophenone ketyl immediately prior to each use. *N*-isopropylacrylamide (NIPAM) from Eastman Kodak was recrystallized three times from a benzene/*n*-hexane mixture prior to use. *N*, *N*-methylenebisacrylamide (MBA) from Sinopharm was purified by recrystallization from methanol. 2-dodecylsulfanylthiocarbonylsulfanyl-2-methyl propionic acid (DMP) was prepared as described before [19]. Other reagents were purchased from Sinopharm and used without further purification unless noted otherwise.

B. Laser light scattering and zeta potential measurements

A commercial laser light scattering (LLS) spectrometer (ALV/DLS/SLS-5022F) equipped with a multi-τ digital time correlator (ALV5000E) and a cylindrical 22 mW UNIPHASE He-Ne laser (λ_0=632.8 nm) as the light source was used. In dynamic LLS [20], the Laplace inversion of each measured intensity-intensity time correlation function $G^{(2)}(q,t)$ in the self-beating mode can lead to a line-width distribution $G(\Gamma)$, where q is the scattering vector. For dilute solutions, Γ is related to the translational diffusion coefficient D by $(\Gamma/q^2)_{q\to 0,C\to 0}\to D$. Therefore $G(\Gamma)$ can be converted into a translational diffusion coefficient distribution $G(D)$ or further a hydrodynamic radius distribution $f(R_h)$ using the Stokes-Einstein equation,

$$R_h = \frac{k_B T}{6\pi\eta_0 D} \tag{1}$$

where k_B, T, and η_0 are the Boltzmann constant, the absolute temperature, and the solvent viscosity, respectively. In all the LLS experiments, the solutions were clarified with 0.45-μm Millipore Millex-LCR filters to remove dust. Zeta potential measurements of core-shell nanogels with a concentration of 0.1 mg/mL were carried out on a Malvern Zetasizer Nano ZS instrument. The pH of the solution was adjusted using 10 mmol/L HCl or 1 mmol/L KOH.

C. Gel permeation chromatography

The relative molecular weight and molecular weight distribution were measured on a Waters 515 Gel permeation chromatography (GPC) equipped with Ultrahydrogel columns using PEO as the calibration standard. Elution was performed at 35 °C using an aqueous buffer (0.05 mol/L $NaHCO_3$ and 100 mmol/L $NaNO_3$) at a flow rate of 1.0 mL/min.

D. Synthesis of poly(acrylic acid) macro-CTA

In a typical experiment, AA (10.00 g, 0.139 mol), DMP (3.64 g, 10 mmol), 1,4-dioxane (20.0 mL), and AIBN (16.4 mg, 0.1 mmol) with the molar ratio of AA/DMP/AIBN 1390:100:1 were charged into a 50 mL Schlenk flask. After three freeze-pump-thaw cycles, the flask was placed in a preheated oil bath at 80 °C for 6 h. The flask was immediately immersed into liquid nitrogen to stop the polymerization. The resulting PAA macro-CTA was obtained by precipitation of polymerization mixture into excess diethyl ether under filtration and vacuum dryness at room temperature overnight. The synthesis route is shown in Fig.1. The number-averaged molecular weight of PAA was determined by ^{1}H NMR analysis. ^{1}H NMR, DMSO-d_6, δ(TMS): 0.88 (m, 3H, CH_3), 1.10−2.32 (m, CH_2CH), 3.31 (t, 2H, CH_2S), 12.25(s, 1H, COOH). The relative molecular weight and molecular weight distribution (M_w/M_n) was determined by gel permeation chromatography. Other PAA macro-CTA samples with higher molecular weights were synthesized similarly by adjusting both the amounts of DMP and AIBN, as shown in Table I.

E. Dispersion polymerization of NIPAM with PAA-DMP

Aqueous dispersion polymerization synthesis was conducted at a solid content of 2%. A typical protocol was as follows: NIPAM (1.00 g), potassium persulfate (KPS, 50 mg), poly(acrylic acid) macro-CTA (80 mg) and K_2CO_3 (80 mg) were codissolved in deionized water (50 g). The reaction mixture was sealed in a round-bottomed flask and purged with nitrogen for 30 min before being placed in a preheated oil bath at 70 °C for 24 h.

DOI:10.1088/1674-0068/25/04/463-468

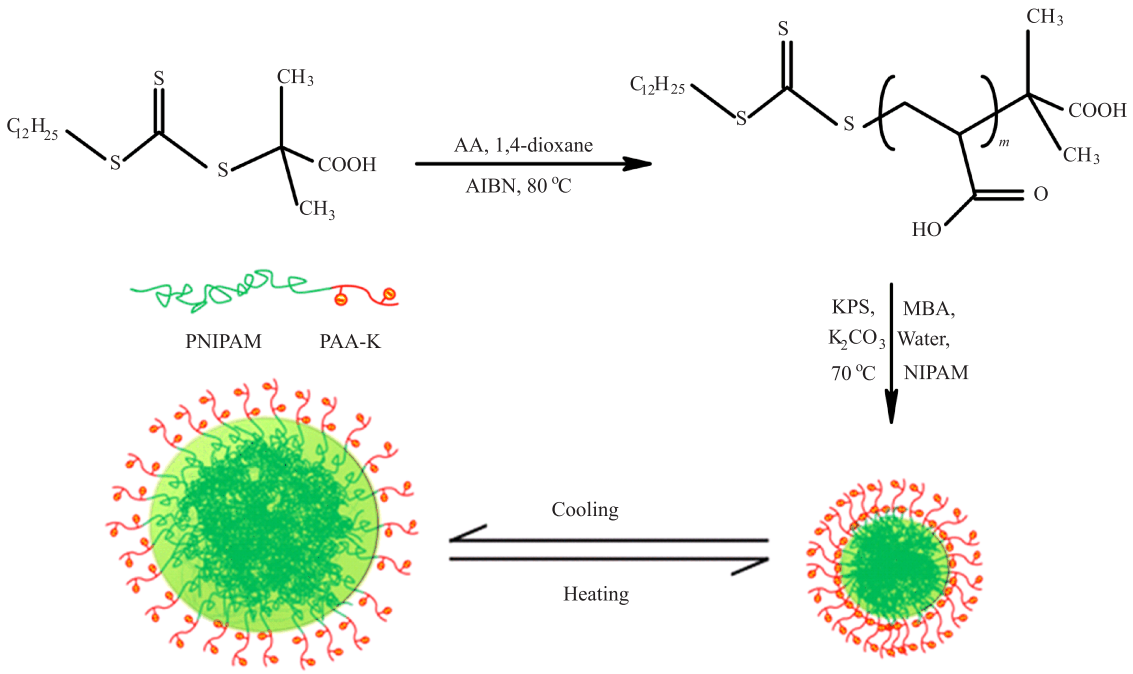

FIG. 1 Synthesis of PAA macro-CTAs and schematic representation of phase transition process.

TABLE II Synthesis results of PAA-PNIPAM nanogels prepared via dispersion polymerization at 70 °C using PAA-K macro-CTA with different molecular weights, 80 mg of PAA, 20 mg of MBA, 80 mg of K_2CO_3, and 50 mg of KPS.

Entry	M_n/(g/mol)	R_h[a]/nm	PD.I
1	2000	60	0.11
2	3800	80	0.05
3	4500	132	0.06

[a] Measured by DLS in water at 25 °C, where the concentration of the nanogel was 0.1 mg/mL.

TABLE III Synthesis results of PAA-PNIPAM nanogels prepared via dispersion polymerization at 70 °C using PAA macro-CTA (M_n of 2000 g/mol) with different concentrations, 20 mg of MBA, 80 mg of K_2CO_3, and 50 mg of KPS.

Entry	PAA/mg	R_h[a]/nm	PD.I
1	40	122	0.11
2	50	73	0.03
3	80	58	0.10

[a] Measured by DLS in water at 25 °C, where the concentration of the nanogel was 0.1 mg/mL

III. RESULTS AND DISCUSSION

A series of well-defined poly(acrylic acid) macro-CTAs were prepared by the RAFT polymerization to investigate the effect of molecular weight of the macro-CTAs on the formation of the nanogels. Typical recipes are given in Table I. Three PAA macro-CTAs were characterization by both GPC and ^{1}H NMR and the corresponding data are summarized in Table I. Note that all PAA macro-CTAs are narrowly distributed and the number average molecular weight measured by GPC is larger than that characterized by ^{1}H NMR [21].

In the dispersion polymerization, RAFT process translates these PAA-K blocks onto the surface when nanogels are prepared. Table II summarizes the recipes for the synthesis of PAA-PNIPAM nanogels using PAA-K macro-CTAs with different molecular weights. The results show that polydispersity index (PD.I) of the obtained PAA-PNIPAM nanogels ranges from 0.05 to 0.11, indicating that they are narrowly distributed. On the other hand, the size of the core-shell nanogels depends on the molecular weight of PAA-K macro-CTA. As shown in Table II, when the molecular weight of macro-CTA increased from 2000 g/mol to 4500 g/mol, the average hydrodynamic radius $\langle R_h \rangle$ of the core-shell nanogels increased from 60 nm to 132 nm. Due to the dependence of molecular weight of PAA macro-CTA on the size of the core-shell nanogels, we can synthesize core-shell nanogels with controlled size by adjusting the molecular weight of PAA macro-CTA.

A series of PAA-PNIPAM nanogels were synthesized in aqueous media by adjusting the amount of PAA macro-CTA. The average hydrodynamic radius of the nanogels decreases from 122 nm to 58 nm as the amount of PAA macro-CTA with M_n of 2000 g/mol increases from 40 mg to 80 mg, as shown in Table III. Suppose each macro-CTA occupies the same area on the surface

DOI:10.1088/1674-0068/25/04/463-468

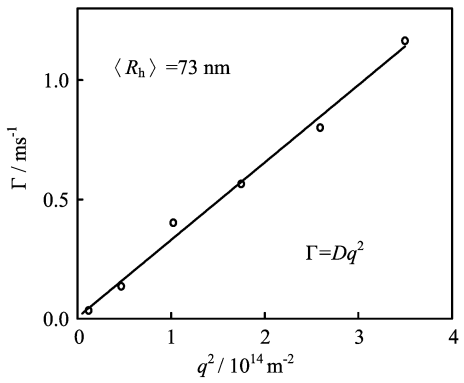

FIG. 2 Scattering vector dependence of the average characteristic line-width, where T=25 °C, the concentration of PAA-PNIPAM nanogel was 0.1 mg/mL and pH=7.2.

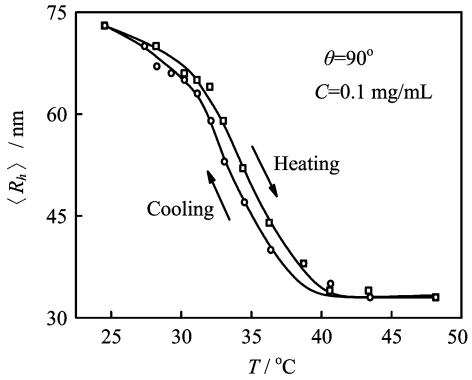

FIG. 3 Temperature dependence of average hydrodynamic radius $\langle R_h \rangle$ of PAA-PNIPAM nanogel in an aqueous solution, where the concentration of the nanogel was 0.1 mg/mL and pH=7.2.

of the particle [22], more macro-CTAs should stabilize more particle surface, thus resulting in smaller microgels. This result is consistent with the results reported in Ref.[14]. In addition, the lower polydispersity of the obtained nanogels shows that PAA acts as a good stabilizer in the formation of core-shell nanogels.

We investigated the phase transition behavior of PAA-PNIPAM core-shell nanogels (entry 2 in Table III) in detail. Figure 2 shows that the average characteristic line-width not only has a linear dependence on q^2, but also passes through the origin as $q \to 0$, indicating that the relaxation is diffusive. This angular independence indicates a spherical symmetry of the nanoparticles. From the slope we know that the average hydrodynamic radius $\langle R_h \rangle$ of the PAA-PNIPAM nanogels is 73 nm when the solution temperature is 25 °C.

Figure 3 shows that the shrinking and swelling of the resultant core-shell nanogels (entry 2 of Table III) in the heating and cooling cycle are reversible. An obvious hysteresis was observed during the heating-and-cooling cycle, which can be attributed to the formation of some additional intrachain hydrogen bonds when PNIPAMs

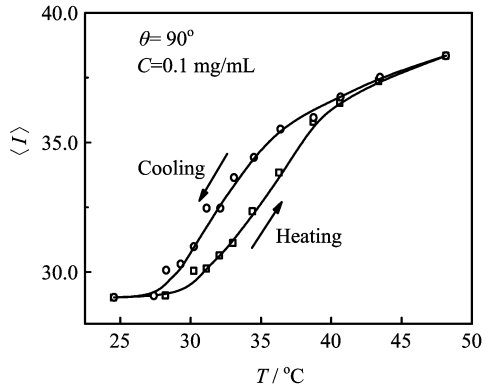

FIG. 4 Temperature dependence of average scattered light intensity $\langle I \rangle$ of PAA-PNIPAM nanogel in an aqueous solution, where the concentration of the nanogel was 0.1 mg/mL and pH=7.2.

are in its collapsed state [23−29]. When the temperature changes from 25 °C to 45 °C, the average hydrodynamic radius decreases from 73 nm to 33 nm; *i.e.*, we can change the grafting density just by varying the solution temperature.

Figure 4 shows the average scattered light intensity $\langle I \rangle$ of the core-shell nanogel as a function of temperature, where θ=90° and C=0.1 mg/mL. When the temperature varied, the change of $\langle I \rangle$ is attributed to the temperature dependence of dn/dC and the size change of the nanogels [30]. The scattered light intensity is reversible in the heating and cooling cycle, which is consistent with the result shown in Fig.3. Moreover, the hysteresis of scattered light intensity is also attributed to the formation of some additional intrachain hydrogen bonds when PNIPAM are in its collapsed state.

Our results show that the weight average molar masses of the core-shell nanogel ($\langle M_w \rangle \approx 2.5\times10^7$ g/mol) slightly change as the temperature increases, that is, no aggregation occurs when PNIPAM core collapses. On the basis of the $\langle M_w \rangle$ of the nanogels and the results from Fig.3, using a simple approximation:

$$\langle \rho \rangle \approx \frac{\langle M_w \rangle}{N_A (4/3)\pi \langle R_h \rangle^3} \tag{2}$$

we can calculate $\langle \rho \rangle$ at different temperatures, as shown in Fig.5. The results show that $\langle \rho \rangle$ increases as increasing temperature, revealing that the nanogel becomes more compact. From Fig.5, we know that $\langle \rho \rangle$ is ∼0.3 g/mL at T=48 °C, indicating that the core-shell nanogel still contains ∼70% of water [31]. Besides, the hysteresis of the average chain density is attributed to the formation of some additional intrachain hydrogen bonds when PNIPAMs are in its collapsed state.

It is well known that poly(acrylic acid) as a weak polyelectrolyte can change its chain conformation when the ionic strength or pH is alternated because of the protonation-deprotonation equilibrium of its carboxylate groups in aqueous solution. The pH of the nanogels

DOI:10.1088/1674-0068/25/04/463-468

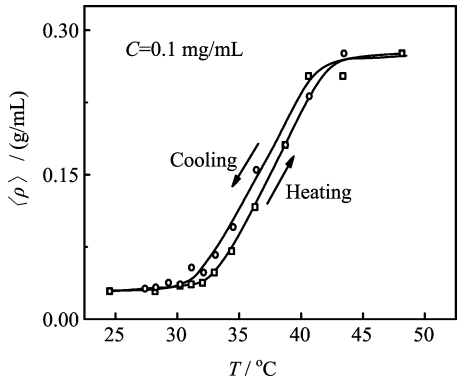

FIG. 5 Temperature dependence of average chain density $\langle\rho\rangle$ of PAA-PNIPAM nanogel in an aqueous solution, where the concentration of nanogel was 0.1 mg/mL and pH=7.2.

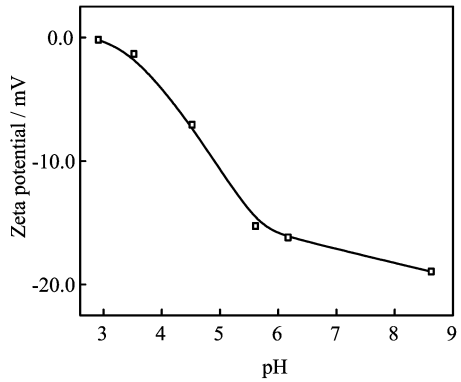

FIG. 6 pH dependence of zeta potential of PAA-PNIPAM nanogels grafted with linear PAA chains, where the concentration of nanogel was 0.1 mg/mL and T=25 °C.

solution was adjusted with HCl and KOH solution and the zeta potentials of the nanogel at different pH values were measured, as shown in Fig.6. The results show that zeta potential is ∼0 mV at pH=3 and decreases to −15.4 mV at pH=6. Further increase in pH only changes the zeta potential slightly. Figure 6 also reveals that the core-shell nanogel has pH sensitivity.

Figure 7 shows the temperature dependence of the zeta potential of the core-shell nanogels. The results show that the zeta potential of nanogels decreases from −19.0 mV to −34.0 mV when the solution temperature increased from 25 °C to 45 °C. The negative value of zeta potential is mainly caused by the COO^- groups in the shell. The decrease in the zeta potential may be due to the increase in the surface charge density because of the shrinking of the nanogels.

IV. CONCLUSION

In this work, we have successfully prepared well-defined, pH and temperature sensitive core-shell nanogels using trithiocarbonated PAA-K as the reactive stabilizer via a simple aqueous dispersion polymerization step. The size of the nanogels can be adjusted by both the weight ratio of PAA-K stabilizer to NIPAM monomer and the molecular weight of PAA-K. DLS measurements show that these core-shell nanogels are narrowly distributed. In a heating and cooling cycle, the shrinking and swelling of the nanogels are reversible. The average hydrodynamic radius of the nanogels decreases steadily with increasing temperature. In the temperature range of 25−45 °C, the nanogels can shrink ∼2.3 times in its average hydrodynamic radius. Besides, the zeta potentials exhibit a strong dependence on both temperature and pH value of the nanogels solution, indicating the existence of both pH and temperature sensitivity.

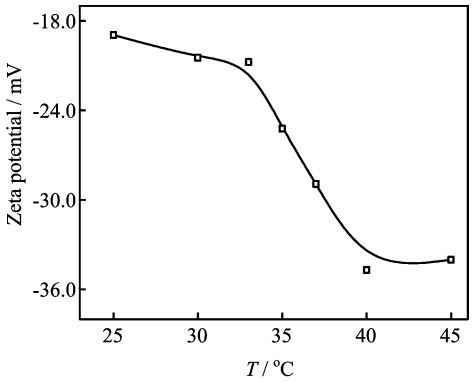

FIG. 7 Temperature dependence of zeta potential of PAA-PNIPAM core-shell nanogels, where pH=8.6 and the concentration of nanogel was 0.1 mg/mL.

V. ACKNOWLEDGMENT

This work was supported by the Scientific Research Foundation for the Returned Overseas Chinese Scholars, State Education Ministry.

[1] J. K. Oh, R. Drumright, D. J. Siegwart, and K. Matyjaszewski, Prog. Polym. Sci. **33**, 448 (2008).
[2] J. M. Weissman, H. B. Sunkara, A. S. Tse, and S. A. Asher, Science **274**, 959 (1996).
[3] R. Pelton, Adv. Colloid Interface Sci. **85**, 1 (2000).
[4] C. E. Reese, A. V. Mikhonin, M. Kamenjicki, A. Tikhonov, and S. A. Asher, J. Am. Chem. Soc. **126**, 1493 (2004).
[5] T. T. Chastek, A. Wadajkar, K. T. Nguyen, S. D. Hudson, and T. Q. Chastek, Colloid. Polym. Sci. **288**, 105 (2010).
[6] K. Otake, H. Inomata, M. Konno, and S. Saito, Macromolecules **23**, 283 (1990).
[7] K. Kubota, S. Fujishige, and I. Ando, J. Phys. Chem. **94**, 5154 (1990).
[8] C. Wu and S. Q. Zhou, Macromolecules **30**, 574 (1997).

DOI:10.1088/1674-0068/25/04/463-468

[9] S. Q. Zhou and B. Chu, J. Phys. Chem. B **102**, 1364 (1998).
[10] H. Senff and W. Richtering, J. Chem. Phys. **111**, 1705 (1999).
[11] K. Kratz, T. Hellweg, and W. Eimer, Colloids Surf. A **170**, 137 (2000).
[12] R. H. Pelton and P. Chibante, Colloids Surf. **20**, 247 (1986).
[13] J. Rieger, C. Grazon, B. Charleux, D. Alaimo, and C. Jerome, J. Polym. Sci. A **47**, 2373 (2009).
[14] Z. An, Q. Shi, W. Tang, C. K. Tsung, C. J. Hawker, and G. D. Stucky, J. Am. Chem. Soc. **129**, 14493 (2007).
[15] G. Delaittre, M. Save, and B. Charleux, Macromol. Rapid Commun. **28**, 1528 (2007).
[16] M. Semsarilar, V. Ladmiral, A. Blanazs, and S. P. Armes, Langmuir **28**, 914 (2011).
[17] W. D. He, X. L. Sun, W. M. Wan, and C. Y. Pan, Macromolecules **44**, 3358 (2011).
[18] J. Kim, H. Jeon, K. Lee, J. Im, and J. Youk, Fibers and Polymers **11**, 153 (2010).
[19] J. T. Lai, D. Filla, and R. Shea, Macromolecules **35**, 6754 (2002).
[20] B. Berne and R. Pecroa, *Dynamic Light Scattering*, New York: Plenum Press, 1 (1976).
[21] J. Loiseau, N. Doërr, J. M. Suau, J. B. Egraz, M. F. Llauro, C. Ladavière, and J. Claverie, Macromolecules **36**, 3066 (2003).
[22] Q. Song, G. Zhang, and C. Wu, Acta Polym. Sin. **25**, 1006 (2007).
[23] L. Shen and G. Z. Zhang, Chin. J. Polym. Sci. **27**, 561 (2009).
[24] Y. Ding and G. Zhang, Macromolecules **39**, 9654 (2006).
[25] H. Cheng, L. Shen, and C. Wu, Macromolecules **39**, 2325 (2006).
[26] G. M. Liu and G. Z. Zhang, J. Phys. Chem. B **109**, 743 (2005).
[27] Y. Maeda, T. Nakamura, and I. Ikeda, Macromolecules **34**, 1391 (2001).
[28] Y. Maeda, T. Higuchi, and I. Ikeda, Langmuir **16**, 7503 (2000).
[29] C. Wu and X. Wang, Phys. Rev. Lett. **80**, 4092 (1998).
[30] C. Wu and S. Q. Zhou, J. Macromol. Sci. Phys. B **36**, 345 (1997).
[31] C. Wu, Polymer **39**, 4609 (1998).

DOI:10.1088/1674-0068/25/04/463-468